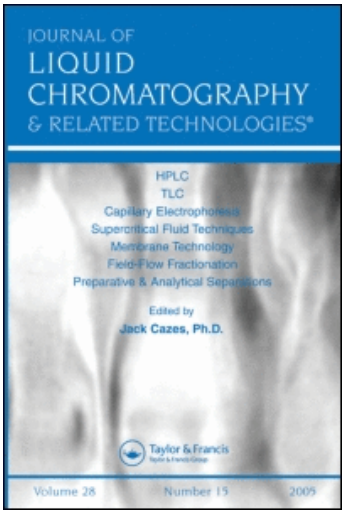

Journal of Liquid Chromatography & Related Technologies
Publication details, including instructions for authors and subscription information:
http://www.informaworld.com/smpp/title~content=t713597273

Synthesis and Characterization of Silica-Immobilized Serum Albumin Stationary Phases for HPLC

V. Tittelbach[ab]; M. Jaroniec[a]; R. K. Gilpin[a]
[a] Separation and Surface Science Center Department of Chemistry, Kent State University, Kent, Ohio [b] Agricultural Research Division American Cyanamid Company Princeton, NJ

To cite this Article Tittelbach, V. , Jaroniec, M. and Gilpin, R. K.(1996) 'Synthesis and Characterization of Silica-Immobilized Serum Albumin Stationary Phases for HPLC', Journal of Liquid Chromatography & Related Technologies, 19: 17, 2943 — 2965
To link to this Article: DOI: 10.1080/10826079608015119
URL: http://dx.doi.org/10.1080/10826079608015119

J. LIQ. CHROM. & REL. TECHNOL., 19(17&18), 2943-2965 (1996)

SYNTHESIS AND CHARACTERIZATION OF SILICA-IMMOBILIZED SERUM ALBUMIN STATIONARY PHASES FOR HPLC

V. Tittelbach,[1] M. Jaroniec, R. K. Gilpin

Separation and Surface Science Center
Department of Chemistry
Kent State University
Kent, Ohio 44242

[1]Current address:
Agricultural Research Division
American Cyanamid Company
Princeton, NJ 08543

ABSTRACT

Chiral HPLC stationary phases based on immobilized biopolymers (i.e., proteins, enzymes, antibodies etc.) are of growing importance for the separation and purification of enantiomeric compounds, especially in the areas of biological, pharmaceutical, and clinical chemistry. In the work described in this paper, several silica-immobilized serum albumin phases were synthesized and characterized by a variety of techniques. Low-temperature nitrogen adsorption isotherms were measured and employed to evaluate the surface characteristics of the stationary phases as a function of both the immobilization matrix and the surface modification chemistry. Elemental analysis and high resolution thermogravimetry were used to evaluate the surface coverages at each stage of modification. Based on these results,

surface parameters such as the specific surface area, pore size distribution, bonding density, etc. were calculated, as well as the changes of these parameters as a function of the modification chemistry were analyzed. Different silicas of varying mean pore diameter from 30 nm to 400 nm were used.

INTRODUCTION

One of the fastest expanding areas of liquid chromatography is the separation of enantiomers using direct methods[1] (i.e., using chiral selective stationary phases). While a large number of applications of protein phases have been published, a majority of the work has focused on more practical aspects of the separation. On the other hand, mechanistic considerations often have not been elucidated fully.

In the field of chiral HPLC a significant improvement in the performance of protein based columns was achieved with the introduction of silica as the support matrix.[2] The advantages of using silica, compared to agarose and other commonly employed matrices for biochemical separations, are better mechanical stability and highly reproducible geometrical features, such as particle shape and diameter as well as pore size distribution. Likewise, the modification chemistry for altering the surface of the silica is well established. However, pH instability as well as chemical and energetic heterogeneity of silica-based stationary phases are potential problems.

It is important for the optimization of a separation , as well as for the development of new stationary phases, to fully understand the mechanisms which governs the solute's retention. Such knowledge makes it possible to take advantage of, or to exclude, certain forces in order to control the separation process. This is particularly true for protein-based chiral stationary phases (CSPs) due to the intrinsically higher heterogeneity of this type of packing. Thus, the purpose of the current study has been to investigate various parameters that influence the physicochemical properties of a specific class of CSPs, silica-immobilized serum albumins.

There are a number of protein-based CSPs commercially available. The most important ones are silica-based bovine and human serum albumin (BSA and HSA, respectively), α_1-acid glycoprotein (AGP), and ovomucoid (OVM) materials. While AGP CSPs have the broadest utility,[3] immobilized serum albumins are considered to be more important proteins for the separation of neutral and acidic chiral species.[4] Even though only a few different types of protein-based CSPs are commercially available, there are numerous accounts in

the literature which describe other protein phases, such those based on immobilized cellobiohydrolase (CBH-1),[5-7] avidin,[8] trypsin,[9] α-chymotrypsin,[10,11] lysozyme,[12,13] or ovotransferrin.[14] For a general review see Ref. [15]

Except for cases where the protein exhibits very strong interactions with the support matrix, it is necessary to covalently anchor the molecule to the surface.[16,17] Several different pathways of immobilization have been described in the literature. One of the commonly employed techniques involves the use of glutaric dialdehyde as bifunctional reagent to link proteins to amino-derivatized silica. This technique was used in the current study.

Investigations of parameters influencing the chromatographic performance of serum albumin based stationary phases have been reported by several groups. A series of studies have been carried out by Allenmark and coworkers over the years. While their first approaches utilized agarose-immobilized BSA,[16,18] the later work took advantage of the better chromatographic performance of silica-based stationary phases[19,21] and examined various modification techniques and cross-linking agents.[22-24] Other related investigations include the work of Aubel and Rogers,[25,26] who examined the influence of column pretreatment on the enantioselectivity of silica-immobilized BSA phases and that of Dabulis and Klibanov[27] who reported an increase in the binding properties of free BSA in non-aqueous media. However, Gilpin et al.[28] so far have published the only account which describes the use of silica-immobilized BSA in the normal-phase mode. They also found novel applications of this type of stationary phases for GC.[29,30] Additionally, the same group studied the influence of temperature, pH, solute concentration, and other parameters, upon the enantiospecific separation of tryptophan via BSA CSPs.[31-33]

Unlike the above studies which investigated the properties of protein-based CSPs under chromatographic conditions, the current work is focused on the effect of the immobilization chemistry upon the physicochemical properties of the silica matrix via nitrogen adsorption measurements.

MATERIALS

The LiChrospher Si 300 silica (particle diameter 10 μm), which was used to prepare most of the albumin phases, was purchased from EM Separations (Gibbstown, NJ, USA). The other silica samples tested (LiChrospher Si 500, LiChrospher Si 1000, LiChrospher Si 4000, and LiChrospher Si 300 WP), were donated by EM Separations . The γ-aminopropyl triethoxysilane was from

Hüls-America (Piscataway, NJ) and the glutaric dialdehyde (25% solution in water) was from the Aldrich Chemical Co. (Milwaukee, WI, USA). The different serum albumins (i.e., bovine, human, pig, sheep, and horse; essentially fatty acid free), the sodium cyanoborohydride, the sodium phosphate (reagent grade) were obtained from the Sigma Chemical Co. (St. Louis, MO). The deionized water was purified in-house using either a Milli-Q (Millipore, El Paso, TX, USA) or Ionpure Plus 150 (Ionpure, Lowell, MA, USA) reagent water system. All HPLC solvents (HPLC grade), the toluene (ACS specified grade), and the potassium chloride (reagent grade) were from Fisher Scientific (Pittsburgh, PA, USA).

METHODS

Synthesis of Stationary Phases

The silica-immobilized serum albumin stationary phases were prepared according to a modification of a previously reported three-step synthesis.[33] Each step in this procedure was monitored by microcombustion analysis in order to measure the carbon and nitrogen loadings. Initially, the silica was derivatized with γ-aminopropyl triethoxysilane to yield an amino functionality at the surface. An overview of the modification chemistry is given in Figure 1. For steric and probability reasons, most ligands are only anchored to the silica surface via one bond. However, cross-polymerization can yield multiple covalent linkages. For most cases, batches of five grams of each silica were modified at one time. In order to control the amount of physisorbed water at the silica surface, the starting silica was carefully hydrated, followed by a drying step. Specifically designed glass reaction flasks were employed. This was followed by the addition of the γ-aminopropyl triethoxysilane. In steps two and three, the amine surface was first activated, using glutaric dialdehyde as bifunctional reagent, and than the protein was anchored to the silica surface (see reaction scheme in Figure 1). At each step, the progress was monitored by taking a small sample for microcombustion analysis.

Column Packing

Stainless steel columns of dimensions of 15 cm x 0.21 cm I.D. were made from HPLC tubing purchased from Handy & Harman (Norristown, PA, USA). The column blanks were thoroughly cleaned, end fittings were attached and the modified silicas were packed into them using a iso-propanol slurry procedure described previously.[34]

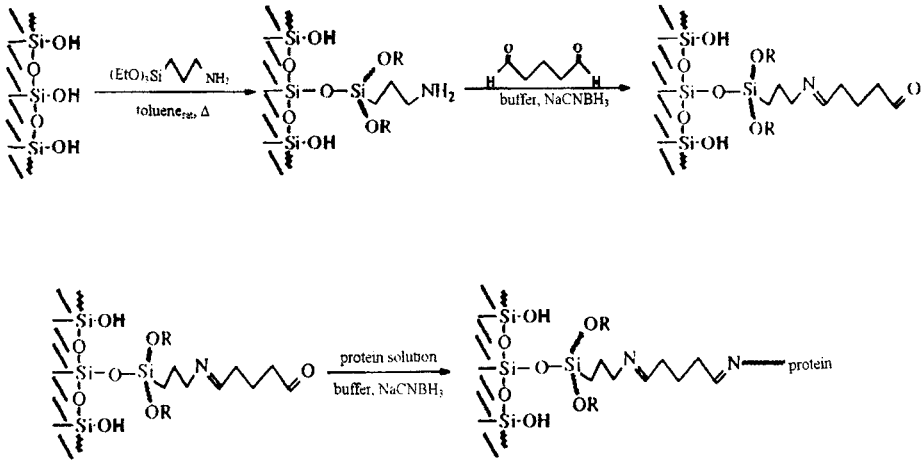

Figure 1. Silica modification chemistry.

The packing system was pressurized to about 6000 psi using a Haskel (Burbank, CA, USA) model DST-162-52 air driven fluid pump. Methanol was used as the carrier solvent, and the packing was continued for around two hours.

Surface Characterization

Each step in the surface modification process was monitored using microcombustion analysis that was carried out, first by Huffman Laboratories (Golden, CO, USA) and later in-house, using a LECO model CHNS-932 (LECO Co., St. Joseph, MI, USA) elemental analyzer. In the latter case, usually three repeats were performed and the results averaged.

The physicochemical properties of the silica samples were evaluated by recording nitrogen adsorption isotherms. The instrument employed was an ASAP 2000 adsorption analyzer (Micromeritics Instrument Corporation, Norcross, GA, USA). Prior to each analysis, the sample tube was carefully washed and dried. About 400 mg of each sample were weighted out and degassed under high vacuum (around 2 μm Hg) for four hours at 100 °C. The final weight was determined after back-filling with analysis gas (dry nitrogen), and then the complete isotherm was recorded at the temperature of liquid nitrogen (i.e., 195.8°C).

Calculations of the BET specific surface area, monolayer capacity, pore size distribution, total pore volume and micropore volume were carried out using the manufacturer's software package.

High resolution thermogravimetric analysis (TGA), was carried out on the stationary phases studied over a range from ambient temperature to 1000 °C, and the degassing temperature was chosen on the basis of these measurements. In doing this, a TA 2950 high resolution analyzer (TA Instruments, Inc., New Castle, DE, USA) was used for studying the thermal properties of the samples.

Chromatographic Measurements

After the packing procedure was complete and prior to carrying out any chromatographic separations, all columns were conditioned overnight at a flow rate of 0.1 mL/min with the aqueous mobile phase. Then, before use, each of the columns was conditioned at the desired flow rate and temperature for another 30 minutes.

Different sets of chromatographic experiments were carried out on either one of two different HPLC systems. One of this was a Spectra Physics (San Jose, CA, USA) liquid chromatograph consisting of a model 8810 precision isocratic pump, a model spectra 100 series variable wavelength UV detector set to 254 nm, and a model 4400 Chromjet integrator, connected to a PC for data collection. The samples were injected using a Rheodyne (Berkeley, CA, USA) model 7125 six-port injection valve, equipped with a 20 μL sample loop and a position sensor that automatically started the runs.

The temperature of the column and the injection valve were controlled to ± 0.1 °C using a Fisher Scientific (Pittsburgh, PA, USA) model 9500 Isotemp refrigerated circulator bath, while the flow rate was monitored via a Phase Separation (Queensferry, Clwyd., UK) model F1080A digital flowmeter. The experiments were carried out by setting the pump to a value corresponding to a measured flow of 1.00 mL/min. (± 0.02).

The other system was a Varian (Walnut Creek, CA, USA) HPLC consisting of a model 9012 series inert gradient pump, a model 9050 programmable UV detector, and a model 9100 autosampler. The temperature of the column was controlled to 20 °C (± 0.2) using a water bath equipped with a Haake (Karlsruhe, Germany) model DC-1 immersion heater/circulator and a Neslab (Portsmouth, NH, USA) model EN-350 Flowthru Cooler.

The flow rate was monitored at the detector outlet, using a Varian Optiflow 1000 digital flow meter. The system was connected to a PC for system control, data collection and manipulation, using the vendor-provided software package.

RESULTS AND DISCUSSION

Elemental Analysis

In order to determine the qualitative and quantitative changes introduced during synthesis, elemental analysis for carbon and nitrogen was carried out and the resulting data were used to evaluate the degree of the surface coverage by using the following relationship:[35]

$$N_1 = \frac{\%C_1}{1200n_{c,1}(MW_1 - 1)} \quad (1)$$

where %C is the experimentally determined value, $n_{c,1}$ is the number of carbon atoms per attached ligand, MW_1 is the molecular weight of the ligand, and N_i is the number of moles of ligand attached in each step.

In doing this, it was assumed, that on average one ethoxy group remained attached to the silane silicon atom after the triethoxysilane reacted. Thus, the ligand introduced in the step 1 had the formula $-Si(OH)(OC_2H_5)(CH_2)_3NH_2$. The same notation is used for the second step (i.e., see Equation 2):

$$N_2 = \frac{\%C_2 N_1 (MW_1 - 1) - 1200N_1 n_{c,1}}{1200n_{c,2} - \%C_2 (MW_2 - 1)} \quad (2)$$

On average, the carbon load after the first step was 1.33%. Hence, the calculated surface coverage according to equation 1 was about 229 μmol ligands per gram sample.

Using the measured 60 m^2/g BET specific surface area of the silica and 8 μmol silanol groups/m^2, this value translates into a calculated coverage density I of about 47% of the available silanol groups. For mono-functional reagents this value is usually lower due to steric reasons.

Table 1

Physicochemical Properties for Serum Albumins

	BSA	HSA	SSA	PSA	ESA
# of C-atoms	2926	2908	2933	2981	2909
# of N-atoms	779	786	780	789	776
MW	66,236.6	66,410.6	66,263.1	66,536.2	65,593.0
% carbon	53.06	52.59	53.16	53.81	53.26
% nitrogen	16.47	16.58	16.49	16.61	16.57

For the second step of modification, the initial deposition of the amine ligand has to be taken into account. Equation 2 was used to calculate the subsequent conversion into the carbonyl intermediate phase. Based on solution reactivities, it was assumed that the activation via the aldehyde proceeded with almost quantitative yield. The average carbon load for the second step was 2.85%.

The amount of immobilized serum albumin was calculated using the differences between the carbon and nitrogen values prior and following the third modification step. These calculations were based on the data shown in Table 1 and can be found in Ref.[33]

Based on the values given in Table 1, the amount of protein immobilized in the third step averaged about 1 μmol per gram silica. The total carbon load for the silica-immobilized serum albumin stationary phases was between 6 and 7 %C, which is reasonable based on the relatively low specific surface area. Additionally, it was found previously[32] that maximizing the amount of protein anchored to the surface does not maximize the separation abilities of the resulting phase. This effect is shown in Figure 2, where the capacity factors for L-kynurenine and L-tryptophan are plotted vs. the normalized surface coverage. Clearly, an optimal protein coverage exists. This optimized modification procedure was used throughout the work.

Thermogravimetric Analysis

High resolution thermogravimetry (TGA) was employed for monitoring the progress of various synthetic steps. This method provides relatively fast results with good accuracy. Figure 3 shows a correlation between the weight

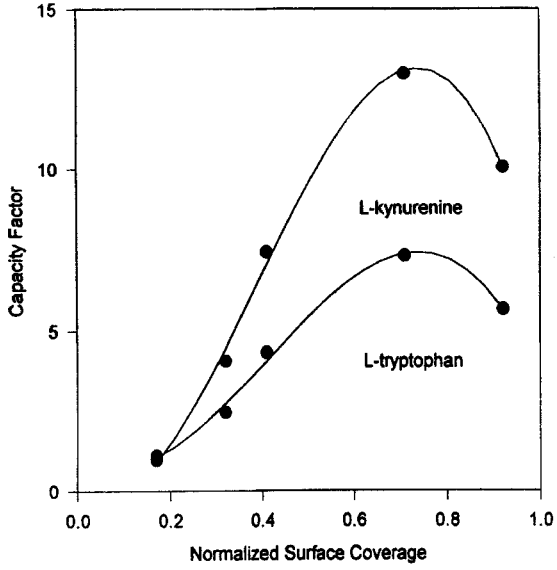

Figure 2. Influence of the BSA coverage on the solute's retention.

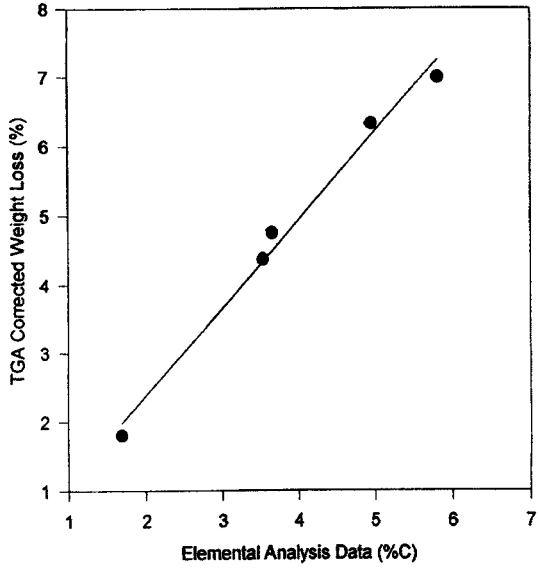

Figure 3. Correlation between the TGA data and elemental analysis.

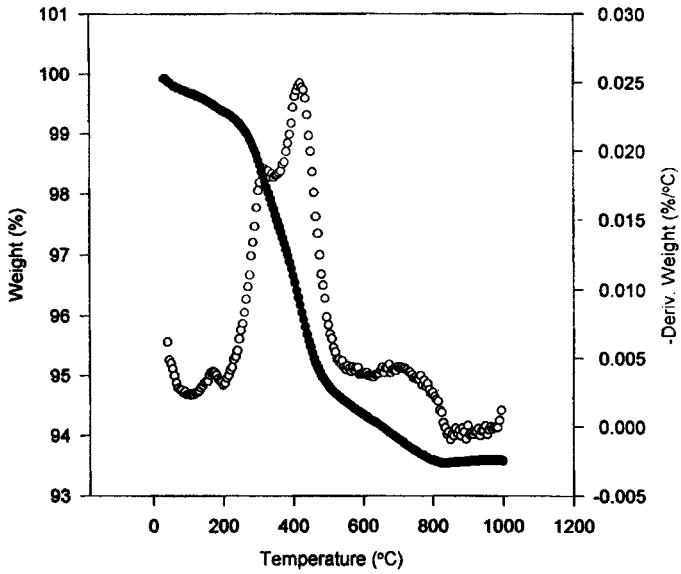

Figure 4. Typical thermogram for a silica-immobilized BSA phase, which contains the weight curve and its first derivative with respect to temperature.

loss, corrected for initial water loss, and the results from elemental analysis. An additional advantage of the TGA-based procedure was that it provides an estimate of the physically sorbed water. A typical thermogram is shown in Figure 4. Initially, up to 200 °C (under inert atmosphere), the physically adsorbed surface water was removed and then, the organic moiety burned off. The weight loss of this step was used to determine an approximate surface coverage, which needed a small correction for the weight loss due to the partial decomposition of residual surface silanols. The oxidation of the ligand was completed around 500 °C. The final loss was due to the condensation of the remaining surface silanol groups. Although this process overlaps the organic oxidation step, the error introduced by it is fairly small.

Influence of the Silica Characteristics on the Surface Coverage

For comparative purposes, four different silicas were used to immobilize BSA. In order to minimize size exclusion effects, all silicas had average pore diameters larger than 250 nm. All materials were modified using the methods described in the experimental section and the surface coverage for each step

was determined using elemental analysis. Additionally, the samples were evaluated via nitrogen adsorption in order to determine the BET specific surface areas. Applying the BET equation for the estimation of the specific surface area is by far the most widely used method.[36,37] By plotting the adsorption data for the relative pressure range of 0.05 to 0.30 according to the BET equation,[37] the monolayer capacity can be determined, which after multiplication by the molecular cross section of the probe molecule (i.e., nitrogen) and Avogadro's number gives the BET specific surface area. A summary of the resulting surface areas of the starting materials as well as the modified silica surfaces is shown in Table 2. All packings investigated were LiChrospher silicas. The Si 300, 1000 and 4000 silicas had an average particle diameter of 10 μm, and the remaining material was 5 μm. Furthermore, the LiChrospher Si 300 WP is a newer type of the 30 nm pore size material, that is called *wide pore* silica. Its specific surface area was slightly higher than the older materials. This increase may be due to the decrease in particle size and other factors.

Except for the Si 300 BSA material, the BET specific surface areas decreased following the BSA immobilization. One might expect that the surface area should increase after protein immobilization, since the BSA molecules might accommodate additional nitrogen molecules at their surface. However, the partial filling of pores (i.e., partial blocking of otherwise accessible surface area) seems to over-compensate this effect.

In addition to the BET specific surface areas, Table 2 contains the average pore sizes for the samples studied. There are different numerical methods available to calculate the average pore size from the nitrogen adsorption data. The values listed in Table 2 were calculated using the software package provided by the manufacturer of the adsorption instrument. These values were obtained on the basis of the pore size distributions calculated by using the BJH method that relates the volume adsorbed to the pore radius through the Kelvin equation.[38] The average pore diameter decreased, as expected, after modification with the exception of the Si 300 material. For the 100 and 400 nm materials, the average pore diameters could not be calculated, since the Kelvin equation is not applicable for materials that contain macropres..

The silica immobilized protein phases studied were tested chromatographically. The separation of D/L-tryptophan was used as a probe to evaluate the chromatographic performance of the synthesized phases. Chromatographic factors influencing that particular separation have been presented previously.[32,33] In the case of the 100 and 400 nm materials. this appears to be a surface area effect. Because of the low surface area available,

Table 2

Physicochemical Characteristics of Modified Silicas

Sample	%C	% N	S_{BET} [m^2/g]	$\overline{D}$ [nm]
Si 300	---	---	60	360
Si 300 amine	1.08	0.37	---	---
Si 300 aldeh.	2.97	0.44	---	---
Si 300 BSA	6.75	1.69	66	375
Si 500	---	---	68	390
Si 500 amine	1.64	0.63	---	---
Si 500 aldeh.	4.29	0.71	---	---
Si 500 BSA	5.81	1.30	66	320
Si 1000	---	---	27	---
Si 1000 amine	1.19	0.34	---	---
Si 1000 aldeh.	2.42	0.43	---	---
Si 1000 BSA	3.53	0.83	25	---
Si 4000	---	---	11	---
Si 4000 amine	0.43	0.09	---	---
Si 4000 aldeh.	1.05	0.13	---	---
Si 4000 BSA	1.69	0.35	9.7	---
Si 300 WP	---	---	84	340
Si 300 WP amine	1.82	0.61	---	---
Si 300 WP aldeh.	4.70	0.73	---	---
Si 300 WP BSA	4.95	1.02	72	280

the amount of immobilized BSA did not provide adequate numbers of binding sites required for enantiomeric separation (i.e., the columns were effectively overloaded). In the case of the 50 and 30 WP materials, it appears that synthesis conditions were not fully optimized. Since, the specific surface area of both starting materials are higher than for the standard 30 nm packing, it is reasonable to expect similar or higher protein coverage, i.e., better chromatographic performance. Also, the particle size of these materials was 5 μm and this factor should further enhance their chromatographic performance.

Interestingly, the coverage following the second modification step was much higher than expected for both silicas. However, the immobilization of the protein did not follow this trend. Contrary, the resulting BSA coverage was lower, compared to the "standard" 30 nm silica.

Influence of the Immobilization Chemistry

Although silica is both energetically and structurally heterogeneous,[39] it is further altered during the various modification steps. Changes in the pore size and energy distributions, which result from the protein modification, influence the chromatographic properties of the CSPs and they can be monitored via adsorption measurements.

Knowledge of the sorption and structural properties and their changes during modification is of great importance for understanding the mechanisms which govern the various chromatographic separations. A study of the sorption characteristics of serum albumin based CSPs was undertaken as an attempt to determine the physicochemical properties of the material at each step of the modification.

The complete (i.e., adsorption and desorption) isotherms shown in Figure 5 can be considered as type IV according to the common classification.[37] In the region of lower relative pressures, they reflect the formation of the monolayer, followed by multilayer adsorption. However, at high relative pressures ($p/p_0 > 0.8$) capillary condensation was observed. All of the isotherms show the same kind of hysteresis loop and its shape was not affected significantly by the subsequent steps of modification. The hysteresis loops resemble type H1, which has the adsorption and desorption branches almost vertical and nearly parallel over an appreciable range of relative pressures.[37] Type H1 of the hysteresis loop is observed for agglomerates made up of spheroidal particles of uniform size and shape. This is in good agreement with the manufacturer's claim of spherical particles with a narrow particle size distribution.

In order to examine the differences in the surface and structural properties of the unmodified silicas, intermediate materials and the final protein phases, a more detailed analysis of these isotherms was carried out. This analysis included the evaluation of the BET monolayer capacity (v_m), the BET specific surface area (S_{BET}), the total pore volume (V_t), the micropore volume (V_{mi}), and the average pore size ($\overline{D}$) for all surfaces. The results are shown in Table 3. The BET monolayer capacity and the BET specific surface area were calculated according to the BET equation by using the nitrogen adsorption data for the

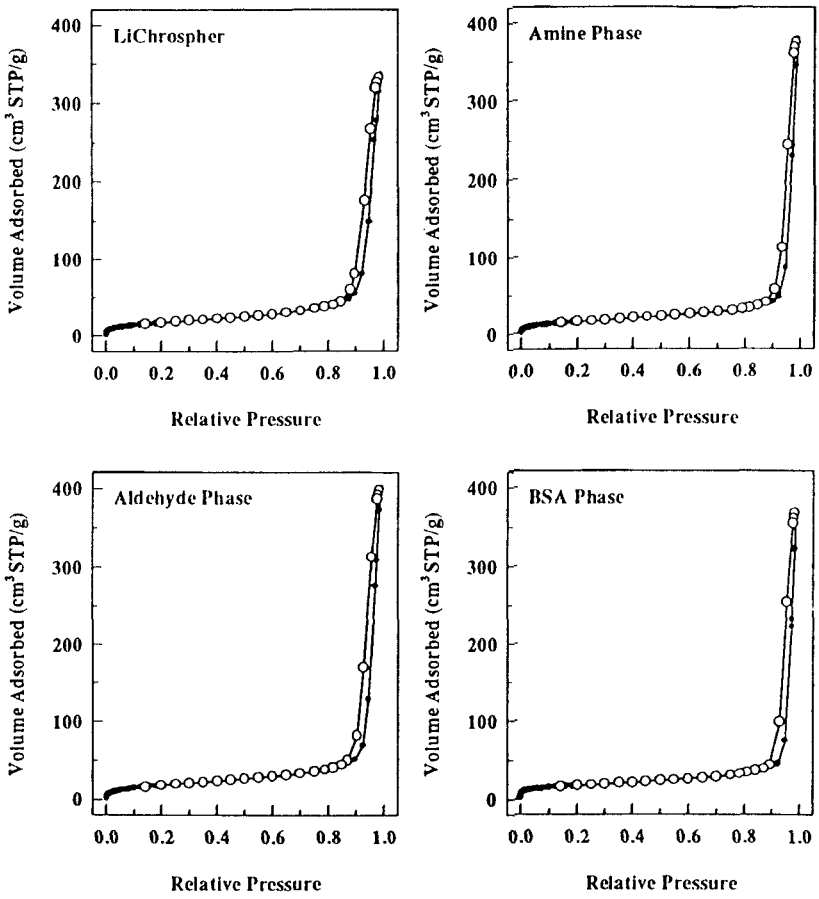

Figure 5. Complete isotherms for low temperature nitrogen adsorption on the starting material (LiChrospher 300), intermediate phases, and silica-immobilized BSA phase.

relative pressure range of 0.05 to 0.25. The total pore volume was evaluated from a single point measured at the relative pressure of about 0.975. The micropore volume, i.e., the volume of pores below 2 nm, was estimated by using the t-plot method,[37] which compares the adsorption isotherm studied with that measured on a nonporous reference material . For further discussion of the t-plot method see ref.[37] The average pore diameter ($\overline{D}$) was derived numerically from the adsorption isotherm using the BJH method developed by Barett, Joyner, and Halenda, which is based on the Kelvin equation.[38]

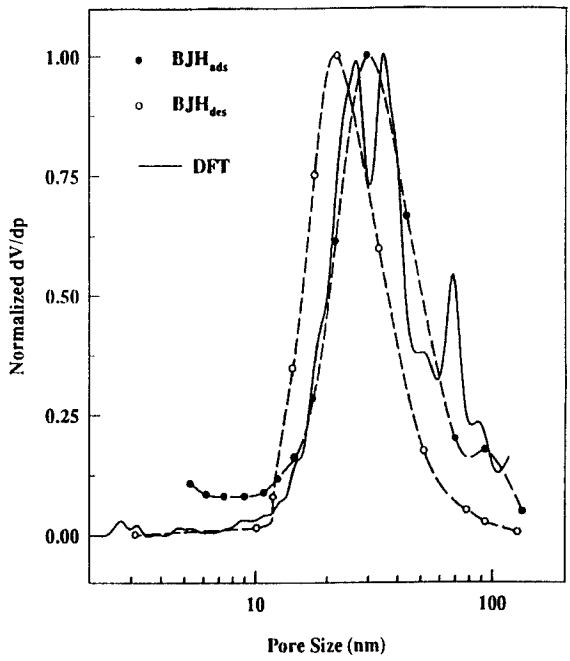

Figure 6. Normalized pore size distributions for Lichrospher Si 300

Table 3

Sorption Parameters of all Silica Surfaces Studies

Sample	V_m [cm^3 STP/g]	S_{BET} [m^2/g]	V_t [cm^3/g]	V_{mi} [cm^3/g]	$\overline{D}$ [nm]
LiChrospher Si 300	14.7	69	0.39	0.004	28.7
Amine Phase	12.8	56	0.35	0.004	25.3
Aldehyde Phase	15.6	68	0.43	0.005	25.1
BSA Phase	13.8	60	0.34	0.008	22.7

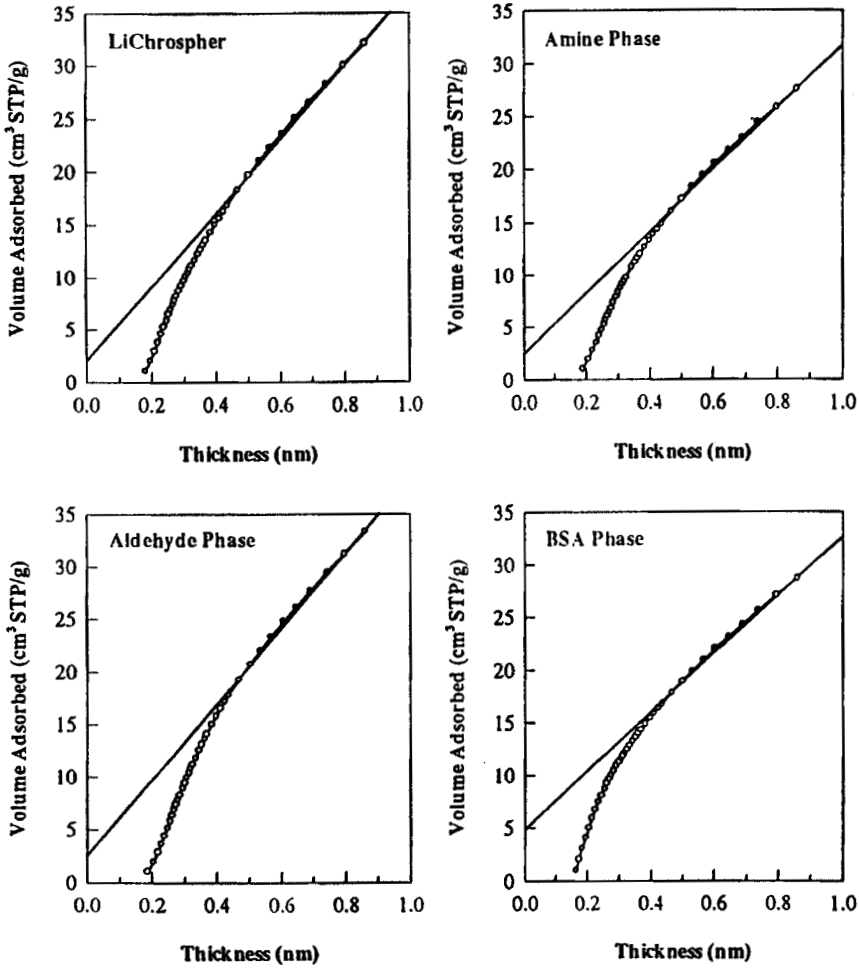

Figure 7. The t-plots for the starting material (LiChrospher 300), two intermediate phases and the BSA phase.

The data in Table 3 show that the micropore volume for all samples analyzed is negligible, as expected. Since the increase in this value for the BSA phase cannot be due to changes in the rigid structure of the support matrix, it has to be due to increased nitrogen adsorption capacity after protein immobilization. Since ligands were anchored to the surfaces during purification modification, the pore size was expected to decrease. The calculated values of the average pore diameter decrease as anticipated.

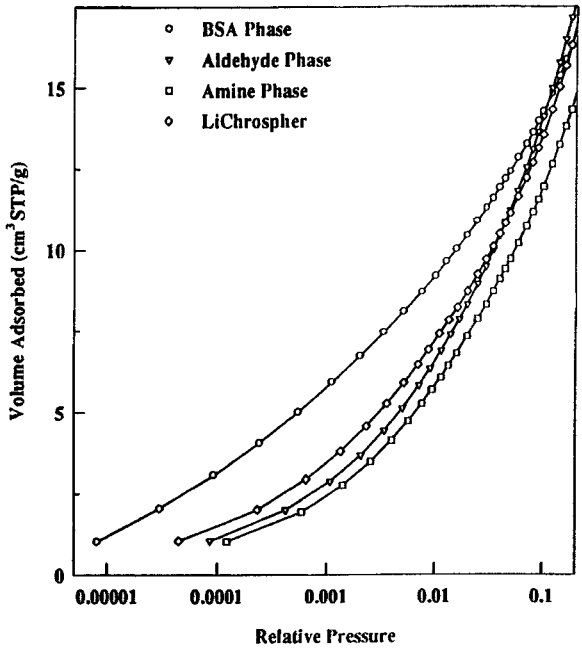

Figure 8. Low pressure branches of nitrogen adsorption isotherms for LiChrospher 300 and other phases studied

Accordingly, the pore diameter decreased from approximately 29 nm for the starting material (30nm according to the manufacturer's specification) to about 23 nm for the protein modified packings. In addition, the pore width data were estimated by an advanced computational method, which utilizes the incremental pore volume distribution obtained by combining the density functional theory (DFT) calculations for the local isotherm with a regularization method.[40]

The initial decrease in the BET surface area (and monolayer capacity) and the subsequent increase following the protein immobilization seem to be reasonable. However, the relatively high values of both parameters for the aldehyde phase cannot be explained conceivably.

Shown in Figure 6 is a comparison of the incremental pore volume distributions obtained by the BJH method with the DFT results for the starting silica matrix. Overall, there is a satisfactory agreement between the pore volume distributions obtained by various methods.

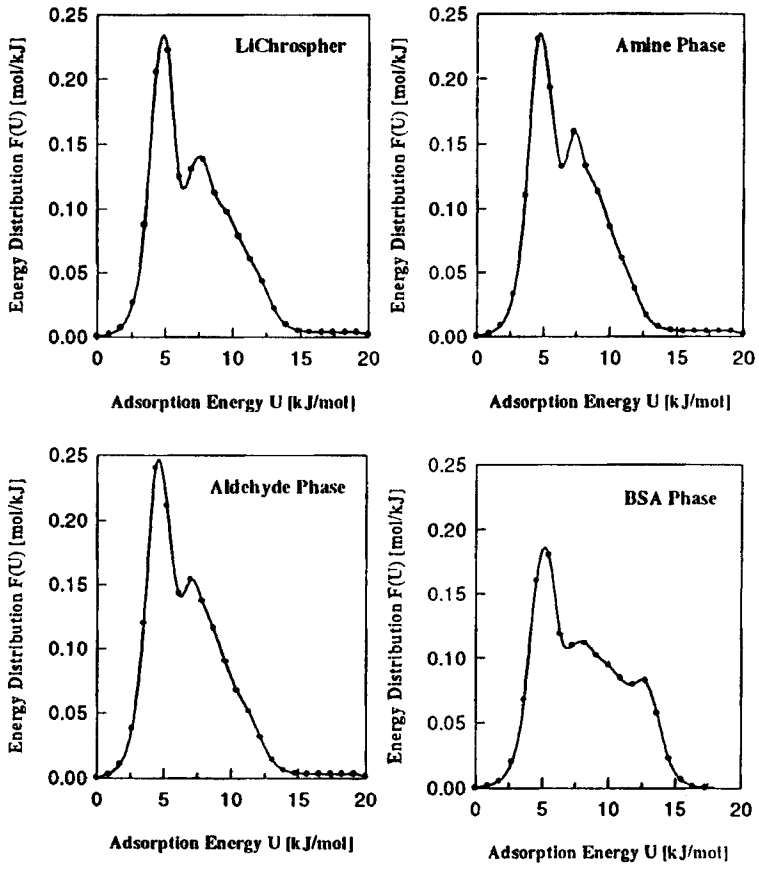

Figure 9. Adsorption energy distributions for LiChrospher 300 and other phases calculated from low temperature nitrogen adsorption isotherms.

It is important to note, however, that the DFT method was developed for the slit-like pore geometry, which is not optimal for sorbents like silica gels. The t-plot is a comparative method which was used to evaluate the microporosity of sorbents.[37] The t-plots for all phases studied are shown in Figure 7. There is no significant difference between these plots. A comparative plot of the low pressure regions for all four isotherms also is given in Figure 8. The branch corresponding to the BSA phase is distinctively different from the others. The amounts adsorbed by the BSA phase at very low

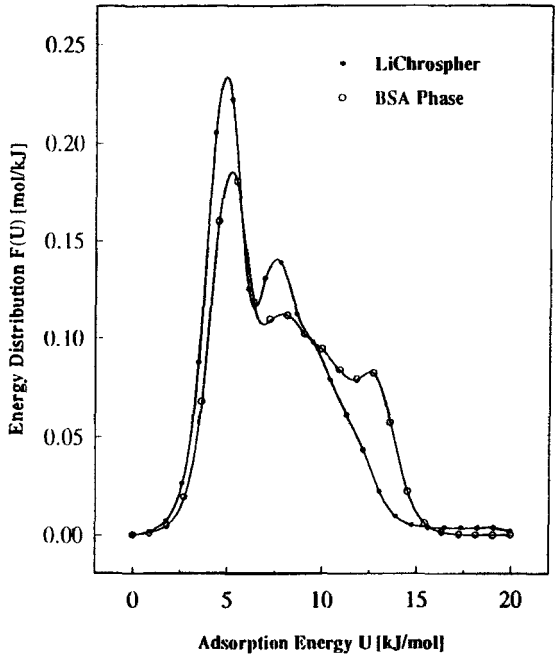

Figure 10. Energy distribution functions for the starting LiChrospher 300 silica (solid circles) and the BSA modified silica (hollow circles).

pressures are greater than those by the starting and intermediate phases. Although this observation can suggest high energetic heterogeneity of this phase, a quantitative comparison of the heterogeneity effects can be done by comparing the energy distributions for the systems studied.

The submonolayer adsorption data were utilized to calculate the adsorption energy distributions for all packings. Again, a regularization method was employed to invert the integral equation of adsorption with respect to the energy distribution.[41]

The energy distribution calculations were performed for the data points below the BET monolayer capacities given in Table 3. All parameters used were set according to previous studies.[42]

The resulting energy distributions for the four surfaces, as calculated from the low pressure nitrogen adsorption data, are shown in Figure 9. These graphs show, that the differences between the distribution curves for the starting silica,

the amine phase, and the aldehyde phase are very small. They have a distinct peak around 5 kJ/mol and a smaller one at about 8 kJ/mol. The smaller peak shows an almost linear tailing to approximately 13 kJ/mol, and a flat contribution in the energy range between 13 and 20 kJ/mol.

It is interesting, that the first and second steps of the silica modification do not change substantially its energetic heterogeneity with respect to nitrogen molecules. It appears, that the replacement of some silanol groups by either aminopropyl or aldehyde groups does not influence the nitrogen adsorption significantly. Other probe molecules could possibly be used to monitor this modification with respect to their adsorption affinities (i.e., argon, methane, benzene or others).

In contrast to the above observation, the BSA anchoring during the third modification step affects the adsorption energy distribution notably in its higher energy portion of the plot, while in the low energy portion it remains unchanged. Figure 10 shows an overlay of the energy distribution functions for the starting silica and the BSA modified silica. These distributions show a main peak around 5 kJ/mol for both phases, however the remaining part of the distribution function is significantly different. Although the smaller peak at 8 kJ/mol is still visible, its tailing is much more complex, exhibiting at least one more maxima at about 13 kJ/mol. A substantial portion of the fraction of sorption sites displaying higher adsorption energies (in the range from 8 to 13 kJ/mol) can be attributed to the energetically diverse structure of the protein. The disappearance of a small fraction in the energy range higher than 13 kJ/mol, however, possibly reflects the blocking of some high-energy silanol binding sites due to the third step of the modification.

ACKNOWLEDGMENT

We would like to acknowledge Dr. Fred Räbel (EM Separations) for the donation of some of the silicas used in this study.

REFERENCES

1. S. G. Allenmark in **Chiral Separations in Liquid Chromatography**, S. Ahuja (ed.), ACS Symposium Series, Washington, 1991, p. 471.

2. S. Allenmark, B. Bomgren, H. Borén, J. Chromatogr., **264**, 63 (1983).

3. I. W. Wainer in **Drug Stereochemistry**, I.W. Wainer (ed.), Marcel Dekker, Inc., New York 1993.

4. H. J. Ritchie, Lab. Pract., **41 (12)**, 13 (1992).

5. P. Erlandsson, I. Marle, L. Hansson, R. Isaksson, C. Pettersson, G. Pettersson, J. Am. Chem. Soc., **112**, 4573 (1990).

6. I. Marle, P. Erlandsson, L. Hansson, R. Isaksson, C. Pettersson, G. Pettersson, J. Chromatogr., **586**, 233 (1991).

7. S. Hjertén, Y.-M. Li, J.-L. Liao, J. Mohammad, K. Nakazato, G. Pettersson, Nature, **356**, 810 (1992).

8. T. Miva, T. Miyakawa, Y. Miyake, J. Chromatogr., **457**, 227 (1988).

9. K. M. Kirkland, K. L. Neilson, D. A. McCombs, J. Chromatogr., **545**, 43 (19991).

10. I. W. Wainer, P. Jadaud, G. R. Schombaum, S. V. Kadodkar, M. P. Henry, Chromatographia, **25**, 903 (1988).

11. S. Thelohan, P. Jaduad, I. W. Wainer, Chromatographia, **28**, 551 (1989).

12. J. Haginaka, T. Murashima, C. Seyama, J. Chromatogr. A , **666**, 203 (1994).

13. W. Su, R. B. Gregory, R. K. Gilpin, J. Chrom. Sci., **31**, 285 (1993).

14. N. Mano, Y. Oda, T. Miva, N. Asakawa, Y. Yoshida, T. Sato, J. Chromatogr., **603**, 106 (1992).

15. S. Allenmark, S. Andersson, J. Chromatogr. A, **666**, 167 (1994).

16. S. Allenmark, B. Bomgren, H. Borén, J. Chromatogr., **237**, 473 (1982).

17. O. R. Zaborsky in **Immobilized Enzymes**, CRC Press, Cleveland 1973.

18. S. Allenmark, B. Bomgren, J. Chromatogr., **316**, 297 (1984).

19. S. Allenmark, B. Bomgren, H. Borén, J. Chromatogr., **316**, 617 (1984).

20. S. Allenmark, S. Andersson, J. Chromatogr. A, **351**, 231 (1994).

21. S. Allenmark, S. Andersson, J. Bojarski, J. Chromatogr., **436**, 479 (1988).

22. R. A. Thompson, S. Andersson, S. Allenmark, J. Chromatogr., **465**, 263 (1989).

23. S. Allenmark, S. Andersson, P. Erlandsson, S. Nilsson, J. Chromatogr., **498**, 81 (1990).

24. S. Andersson, R. A. Thompsson, S. Allenmark, J. Chromatogr., **591**, 65 (1992).

25. M. Aubel, L. B. Rogers, J. Chromatogr., **392**, 415 (1987).

26. M. T. Aubel, L. B. Rogers, J. Chromatogr., **408**, 99 (1987).

27. K. Dabulis, A. M. Klibanov, Biotech. Bioeng., **39**, 176 (1992).

28. W. Zhao, R. K. Gilpin, presented at the 46th Pittsburgh Conference, New Orleans, LA, 1995; paper 959.

29. L. Mayse, R. K. Gilpin, presented at the 46th Pittsburgh Conference, New Orleans, LA, 1995; paper 925.

30. L. Mayse, M.S. Thesis, Kent State University, Kent, OH, 1995

31. R. K. Gilpin, S.E. Ehtesham, R. B. Gregory, *Anal. Chem.*, **63**, 2825 (1991).

32. V. Tittelbach, R. K. Gilpin, Anal. Chem., **67**, 44 (1995).

33. V. Tittelbach, PhD. Dissertation, Kent State University, Kent, OH, 1995.

34. R. K. Gilpin, W. R. Sisco, J. Chromatogr., **194**, 285 (1980).

35. B. Buszewski, M. Jaroniec, R. K. Gilpin, J. Chromatogr. A, **673**, 11 (1994).

36. K. K Unger in **Packings and Stationary Phases in Chromatographic Techniques**, Chromatographic Science Series, vol. 47, K. K. Unger (ed.), Marcel Dekker, Inc., New York, 1990, p. 54.

37. S. J. Gregg, K. S. W. Sing in **Adsorption, Surface Area and Porosity**, Academic Press, London, 1982, p. 41.

38. E. P. Barett, L. S. Joyner, P. P. Halenda, J. Am. Chem. Soc., **73**, 373 (1983).

39. M. Jaroniec, R. Madey, **Physical Adsorption on Heterogeneous Solids**, Elsevier, Amsterdam 1988.

40. J. P. Olivier, W. B. Conklin, M. v. Szombathely, **Determination of Pore Size Distribution from Density Functional Theory: A Comparison of Nitrogen and Argon Results" in Characterization of Porous Solids III**, J. Rouquerol, F. Rodriguez-Reinoso, K. S. W. Sing, K. K. Unger (eds.), Elsevier, Amsterdam, 1992, p. 81.

41. M. v. Szombathely, P. Bräuer, M. Jaroniec, **J. Comput. Chem.**, **13**, 17 (1992).

42. M. Heuchel, M. Jaroniec, R.K. Gilpin, P. Bräuer, M. v. Szombathely, Langmuir, **9**, 2537 (1993).

Received April 2, 1996
Accepted April 25, 1996
Manuscript 4153